JOC The Journal of Organic Chemistry

Article

pubs.acs.org/joc

Synthesis and Properties of Benzothieno[*b*]-Fused BODIPY Dyes

Zuo-Bang Sun, Man Guo, and Cui-Hua Zhao*

School of Chemistry and Chemical Engineering, Key Laboratory of Special Functional Aggregated Materials, Ministry of Education, Shandong University, Jinan 250100, People's Republic of China

Supporting Information

ABSTRACT: Two benzothieno[*b*]-fused BODIPYs, **BT-BODIPY** and **BBT-BODIPY**, in which one parent BODIPY core is fused with one and two benzothieno rings, respectively, were synthesized from BODIPYs substituted with 2-(methylsulfinyl)phenyl at the *β*-position. The first H_2SO_4-induced cyclization and deborylation afforded benzothieno[*b*]-fused dipyrrin derivatives, which can easily complex with $BF_3{\cdot}OEt_2$ to form the desired benzothieno[*b*]-fused BODIPYs. It was revealed that the fusion of the benzothieno ring is more effective at extending conjugation than simple attachment of the 2-(methylthio)phenyl substituent, which presumably results from conformational restriction. Compared with the corresponding unstrained **SPh-BODIPY** and **BSPh-BODIPY**, which contain one and two 2-(methylthio)phenyl groups at the *β*-position, **BT-BODIPY** and **BBT-BODIPY** display red shifted absorption, increased absorptivity, and fluorescence efficiency. Furthermore, the ring fusion is also helpful to increase stability of the formed cation in **BBT-BODIPY**. Thus, **BBT-BODIPY** exhibits very intriguing properties, such as intense absorption and emission in the red region, very sharp emission spectra, and reversible oxidation and reduction potentials.

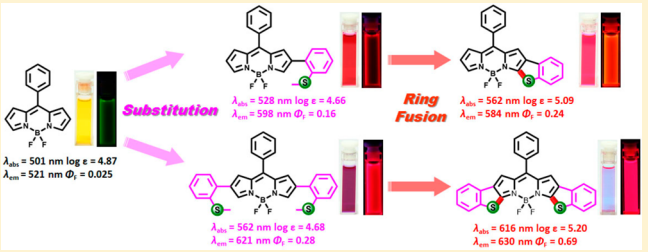

INTRODUCTION

Boradiazaindacenes, commonly known as BODIPY dyes (Figure 1), are one class of the most widely investigated functional chromophores owing to their fascinating properties, such as high photostability, large molar absorption coefficients, sharp fluorescence emissions, and high fluorescence quantum yields.[1] The extensive studies on BODIPY dyes have demonstrated their significant utilities in a broad range of fields, such as chemosensors,[2] photodynamic therapy,[3] laser dyes,[4] emissive materials in OLEDs,[5] and organic photovoltaics.[6] The absorption and emission of classical BODIPY dyes are generally centered in the region of 470−530 nm. However, it is desirable to achieve absorption and emission at longer wavelengths, especially in the red visible to the near-infrared (NIR) range, for the various applications of BODIPY dyes. To this end, several strategies have been adopted to modify the structure of the BODIPY core, such as substitution with aryl,[7] alkynyl,[8] or styryl[9] at peripheral positions, aza-substitution at the *meso*-position,[10] and fusion with aromatic rings.[11] Among them, we are particularly interested in the aryl fusion method. The aryl-fused BODIPYs generally possess more favorable properties than those of unstrained ones due to high rigidity of structures, which would lead to high fluorescence quantum yield in solution and strong *π*-system associations in the solid state. The traditional methods to prepare aryl-fused BODIPY dyes usually required lengthy multistep synthesis of ring-fused pyrroles as starting materials. To circumvent the tedious preparation of ring-fused pyrroles, the direct intramolecular ring closure from peripherally substituted BODIPYs is considered to be a straightforward alternative way. However, such examples are limited to syntheses of several ring-fused BODIPYs, such as benzofuran-fused BODIPYs through palladium catalyzed intramolecular benzofuran formation,[12] perylene- and porphyrin-fused BODIPYs through an oxidative fusion reaction with *meso*-substituents,[13] biphenyl-fused BODIPY via PIFA ([bis-(trifluoroacetoxy)iodo]-benzene)-induced oxidative cyclization of *β*-biphenyl BODIPY,[14] *α*-fused dithienyl BODIPY through $FeCl_3$-induced oxidative ring closure of *β*-dithienyl BODIPY,[15] as well as indole[*b*]-fused BODIPY via reductive Cadogan cyclization of *β*-bis(2-nitrophenyl) BODIPY,[16] or through regioselective nucleophilic substitution of 2,3,5,6-tetrabromo-BODIPY with aryl amine, followed by palladium-catalyzed intramolecular C−C coupling ring fusion.[17] Thus, it still so far remains a challenging issue to obtain asymmetrically fused and heteroaromatic ring[*b*]-fused BODIPYs.

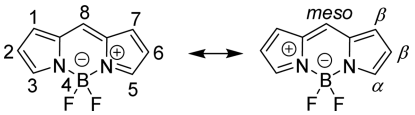

Figure 1. Structure and IUPAC numbering of BODIPY.

In this context, we started to investigate the possibility to prepare benzothieno[*b*]-fused BODIPYs, **BT-BODIPY** and **BBT-BODIPY**, in which one parent BODIPY core is fused with one and two benzothieno rings, respectively (Figure 2),

Received: November 3, 2015
Published: December 4, 2015

DOI: 10.1021/acs.joc.5b02531
J. Org. Chem. 2016, 81, 229−237

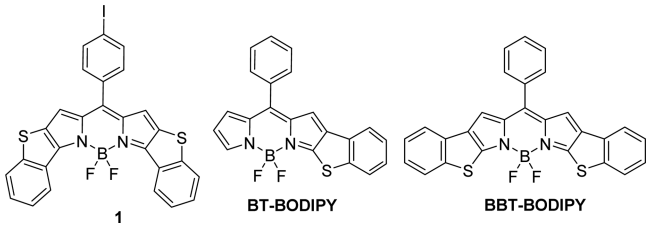

Figure 2. Structure of benzothieno-fused BODIPYs.

through acid-mediated intramolecular cyclization of corresponding *β*-[2-(methylsulfinyl)phenyl]-substituted BODIPY precursors, **SOPh-BODIPY** and **BSOPh-BODIPY** (Schemes 1 and 2). Although the acid-induced cyclization of aromatic methyl sulfoxides has been well utilized to prepare thieno-fused polycyclic aromatics,[18] which are good candidates of semiconductors, the utility of this reaction for the synthesis of ring-fused BODIPY has been unprecedented. The success of this reaction would not only enable preparation of both asymmetric **BT-BODIPY** and symmetric **BBT-BOIDIPY** but also pave a new way to other arenothieno-fused BODIPY analogues that are inaccessible via traditional synthetic methods. In addition, the successful preparation of **BT-BODIPY** and **BBT-BODIPY** will be well complementary to the study of bis(benzothieno)-[*a*]-fused BODIPY **1**.[11a] We envisioned that the fusion of the benzothieno ring with the BODIPY core at the *b*-bond might give rise to some fascinating properties that are quite different from those of corresponding ring[*a*]-fused compounds. Herein, we discuss the synthesis of **BT-BODIPY** and **BBT-BODIPY** from their corresponding methyl sulfoxide precursors, **SOPh-BODIPY** and **BSOPh-BODIPY**, and detailed investigations on their structures, photophysical properties, electrochemical properties, as well as theoretical calculations.

RESULTS AND DISCUSSION

Synthesis. The synthesis was started with the exploration of acid-induced intramolecular cyclization of **SOPh-BODIPY**, which was easily obtained through Pd(0)-catalyzed Suzuki–Miyaura coupling of **2-bromoBODIPY**[19] with 2-(methylthio)-phenylboronic acid, followed by oxidation with hydrogen peroxide (Scheme 1). The ring closure reaction of **SOPh-BODIPY** was carried out in concentrated H_2SO_4. Unexpectedly, the benzothieno[*b*]-fused dipyrrin (DIPY) derivative **BT-DIPY** was obtained instead of **BT-BODIPY** in a moderate yield. The formation of **BT-DIPY** indicated that deborylation also took place during the course of cyclization. The structure of **BT-DIPY** was confirmed by the X-ray crystallography (Figure 3a). Notably, the cyclization took place solely at the *α*-position of the BODIPY core unit. In addition, the benzothieno ring was selectively fused to the pyrrole ring in the structure of

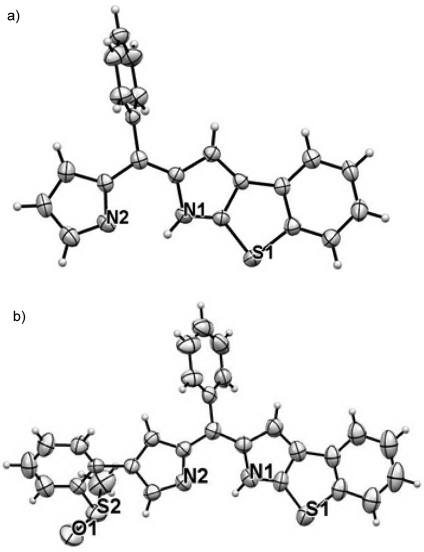

Figure 3. ORTEP drawings of (a) **BT-DIPY** and (b) **SOPhBT-DIPY**. Thermal ellipsoids are drawn at the 50% probability level.

asymmetric **BT-DIPY**. With **BT-DIPY** in hand, the next complexation with $BF_3{\cdot}OEt_2$ proceeded very smoothly to afford the desired **BT-BODIPY** in an almost quantitative yield (94%). As a result, in addition to the benzothieno[*b*]-fused BODIPY derivative, the benzothieno[*b*]-fused dipyrrin derivative was also obtained effectively through this synthetic route. The dipyrrin derivatives are versatile precursors for the synthesis of porphyrins and dipyrrin metal complexes.[20] However, compared with BODIPYs, the parent dipyrrins are more difficult to handle. To enable the functionalization of dipyrrins, BF_2 has recently been used as a masking moiety for dipyrrins. As a consequence, the methods to remove the BF_2 unit from BODIPYs have more recently gained attention. The deborylation of BODIPY can be realized using strong base potassium *tert*-butoxide or Lewis acids such as boron trihalides or $ZrCl_4$.[21]

Considering the significant utility of the deprotection of BODIPY to prepare functionalized dipyrrins, we were interested in whether H_2SO_4 is applicable to the removal of BF_2 for other BODIPY dyes. The deprotection reaction was tested using **2-bromoBODIPY** as a model compound. The starting material **2-bromoBODIPY** disappeared only 5 min after addition of concentrated H_2SO_4, as monitored by thin-layer chromatography. However, nothing was obtained after neutralization of the reaction mixture with aqueous K_2CO_3 and extraction with CH_2Cl_2. The fraction of aqueous phase showed a very deep orange color, implying that **2-bromoBODIPY** might be decomposed to form some water-soluble compounds. These studies suggest that the cationic intermediate formed in

Scheme 1. Synthesis of BT-BODIPY

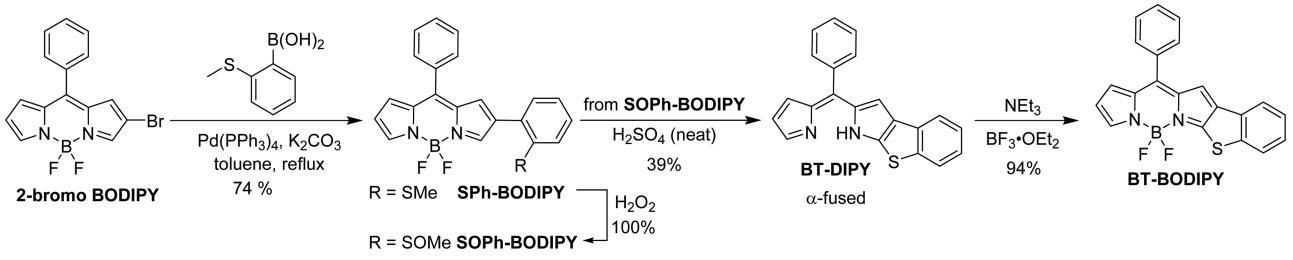

DOI: 10.1021/acs.joc.5b02531
J. Org. Chem. 2016, 81, 229–237

Scheme 2. Synthesis of BBT-BODIPY

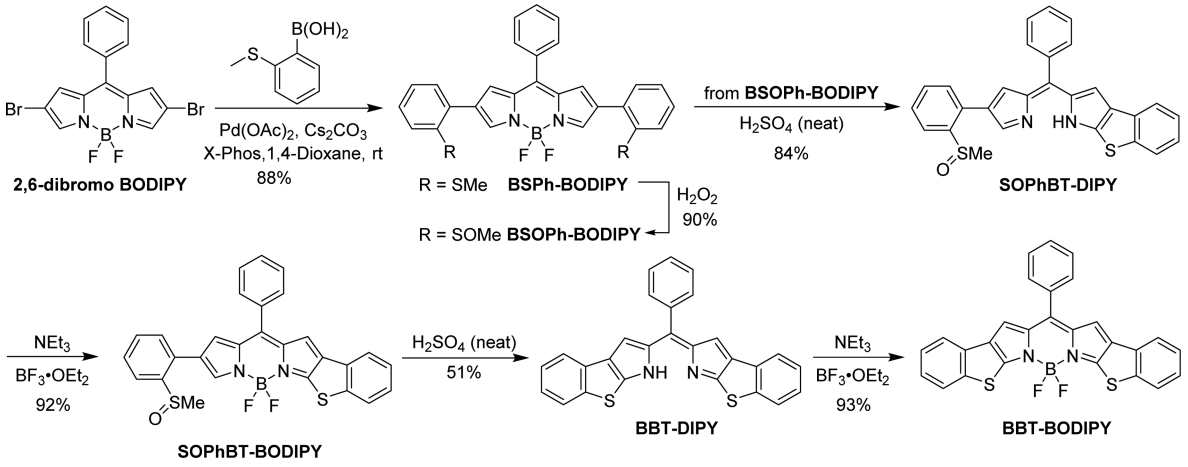

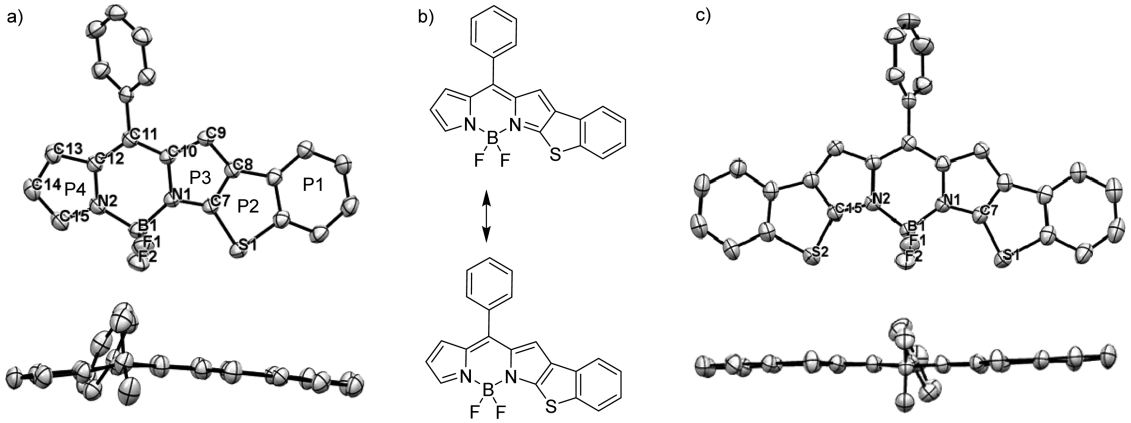

Figure 4. (a) X-ray crystal structure and (b) resonances structure of **BT-BODIPY**. (c) X-ray crystal structure of **BBT-BODIPY**. Thermal ellipsoids are drawn at the 50% probability level. Hydrogens are omitted for clarity.

cyclization of **SOPh-BODIPY** plays an important role to promote the removal of BF_2 unit.

Encouraged by the successful preparation of asymmetric **BT-BODIPY** composed with one benzothieno ring, we next attempted to synthesize symmetric **BBT-BODIPY** formed with two benzothieno rings, using **BSOPh-BODIPY** as the main synthetic precursor. **BSOPh-BODIPY** was synthesized essentially in the same manner as **SOPh-BODIPY** using Suzuki–Miyaura coupling of **2,6-dibromoBODIPY**[19] with 2-methylthiophenylboronic acid and subsequent oxidization by hydrogen peroxide (Scheme 2). In the presence of concentrated H_2SO_4, only one ring was formed in the first step. Similarly, BF_2 was also removed and benzothieno was fused to the pyrrole ring in this step, forming asymmetric benzothieno[*b*]-fused dipyrrin product, **SOPhBT-DIPY**. The structure of **SOPhBT-DIPY** was also confirmed by the X-ray crystallography, as shown in Figure 3b. The difficulty in the simultaneous closure of two benzothieno rings is probably ascribed to the formation of the cationic intermediate, caused by the attack of the first protonic sulfinyl group.[18] The formation of the cationic intermediate will lower the electrophilic substitution reactivity of the BODIPY core and thus suppress the attack from the second protonic sulfinyl group. Subsequently, the facile complexation of **SOPhBT-DIPY** with $BF_3{\cdot}OEt_2$ afforded **SOPhBT-BDOIPY**, which was finally transformed to **BBT-BODIPY** via concentrated H_2SO_4-induced cyclization and decomplexation as well as subsequent complexation with $BF_3{\cdot}OEt_2$. During this synthetic process, bis(benzothieno)[*b*]-fused dipyrrin derivative **BBT-DIPY** was obtained as an intermediate. Through the current synthetic method, we have not only successfully synthesized benzothieno[*b*]-fused BODIPYs, **BT-BODIPY** and **BBT-BODIPY**, but also prepared some benzothieno[*b*]-fused dipyrrins, **BT-DIPY**, **SOPhBT-DIPY**, and **BBT-DIPY**, which might find some important applications in the synthesis of functional porphyrins, and metal complexes.

Crystal Structures. The structures of **BT-BODIPY** and **BBT-BODIPY** were both determined by X-ray crystallography. Their single crystals suitable for X-ray crystallography were obtained by slow evaporation of the solution in the mixed dichloromethane/hexane solvent system. The ORTEP drawings are shown in Figure 4.

For convenience, the benzene, thiophene, thieno-fused pyrrole, and another pyrrole rings of **BT-BODIPY**, are labeled as P1–P4, respectively. It was noted that the three fused rings P1–P3 constitute a very rigid plane, in which the torsion angle between two adjacent rings is less than 1.6°. Meanwhile, P4 is twisted out of the mean plane formed by P1–P3 with a relatively large degree. The torsion angle between them is up to 10.8°. As for the *meso*-carbon C11, it is located in the P4 plane. The deviation of C11 from P4 (0.002 Å) is much shorter than that from the mean plane formed by P1–P3 (0.171 Å). In contrast, the boron atom lies in the mean plane formed by P1–P3. The boron atom is deviated from this plane by only 0.013 Å, while the deviation from the P4 plane is up to 0.23 Å. In

DOI: 10.1021/acs.joc.5b02531
J. Org. Chem. 2016, 81, 229–237

addition, it was also noted that the bond lengths (Å) of C15−N2 (1.341(5)), C13−C14 (1.372(5)), C12−C13 (1.412(4)), and C11−C12 (1.406(5)) are very close to those of C7−N1 (1.340(3)), C8−C9 (1.377(3)), C9−C10 (1.411(5)), and C10−C11 (1.393(3) Å), suggesting equivalent contribution of two resonance structures, as shown in Figure 4b. Another notable structural feature for **BT-BODIPY** is that the C7−S1 bond (1.723(2) Å) is substantially shorter than C1−S1 (1.775(4) Å), which probably denotes that the sulfur atom is conjugated with the BODIPY core unit more efficiently than with the terminal phenyl ring.

From **BT-BODIPY** to **BBT-BODIPY**, the entire main chain skeleton becomes more flat. Each benzothienopyrrole moiety forms a very coplanar structure with torsion angles between adjacent rings of less than 1.4°. The torsion angle between these two mean planes is only 1.01°. In addition, C11 is also located in the entire parent skeleton. The deviation of C11 from the whole mean plane composed of two benzothienopyrrole units is only 0.018 Å. Comparatively, the B atom is deviated from the whole mean plane comprising two benzothienopyrrole units more greatly, with a deviation of 0.19 Å. With regard to the structural similarity between **BT-BODIPY** and **BBT-BODIPY**, it was found that the distances between S and the central BODIPY core unit (1.719(3), 1.715(3) Å) are also shorter than those between S and terminal phenyl rings (1.771(4), 1.768(4) Å).

To further elucidate the effect of benzothieno[*b*]-fusion on structures, the NICS(0) values were calculated at the B3LYP/6-31G++(d,p) level for the optimized structures of **BT-BODIPY** and **BBT-BODIPY**, which are summarized in Figure 5. In addition, the NICS(0) values of the parent **BODIPY** core were also calculated for comparison. The optimized structures were obtained by density functional theory (DFT) calculations at the B3LYP/6-31G(d) level. The NICS(0) values of thiophene rings are −4.6 and −5.0 for **BT-BODIPY** and **BBT-BODIPY**, respectively, suggesting the aromatic characteristics of thiophene rings. Compared with pyrrole in **BODIPY**, the NICS(0) values of pyrroles in benzothienopyrrole substructures for **BT-BODIPY** and **BBT-BODIPY** are slightly less lower (−6.8 for **BODIPY**, −5.6 for **BT-BODIPY** and **BBT-BODIPY**). Thus, the fusion of benzothieno does not have much influence on the aromatic characteristics of pyrrole rings. The current results about NICS(0) calculations might suggest highly efficient conjugation extension via the ring fusion in the benzothieno-fused BODIPY system, which is supposed to have great influence on optoelectronic properties.

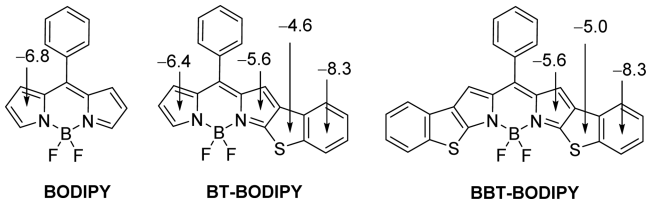

Figure 5. NICS(0) values at the center points of rings for benzothieno[*b*]-fused BODIPYs and related compounds, calculated at the B3LYP/6-31G++(d,p) level.

Photophysical Properties. Both **BT-BODIPY** and **BBT-BODIPY** are intensely colored solids with a metallic luster. Their photophysical properties were first characterized in cyclohexane. The corresponding absorption and emission spectra are shown in Figure 6, and the related data are summarized in Table 1. To elucidate the effect of benzothieno-[*b*]-fusion, the photophysical properties of other related compounds, including unstrained **SPh-BODIPY**, **BSPh-BODIPY**, and the central **BODIPY** core, were also measured for comparison.

In cyclohexane, the **BODIPY** core displays an intense narrow absorption band at 501 nm (log ε = 4.87) with an additional weaker absorption band at shorter wavelength, which are features classic of BODIPY dyes. The attachment of 2-(methylthio)phenyl at the β-position in **SPh-BODIPY** shifts the absorption to 528 nm. The absorption is further red shifted to 560 nm with introduction of another 2-(methylthio)phenyl group in **BSPh-BODIPY**. The significant bathochromism of absorption from BODIPY to **SPh-BODIPY** and further **BSPh-BODIPY** suggests the efficient extension of conjugation induced by the introduction of 2-(methylthio)phenyl. It was noted that the fine structure of absorption spectra is lost in **SPh-BODIPY** and **BSPh-BODIPY**, which may result from free vibration of the 2-(methythio)phenyl group. Most notably, a substantial red shift was observed in absorption with thieno-fusion from unstrained BODIPYs to the strained BODIPYs, which was accompanied by the recovery of fine structure in absorption. The red shifts of absorption from **SPh-BODIPY** to **BT-BODIPY** and from **BSPh-BODIPY** to **BBT-BODIPY** are 34 and 54 nm, respectively. Thus, the absorption of **BBT-BODIPY** (616 nm) already is in the red region. Also noteworthy is that the absorptivity of ring-fused **BT-BODIPY** and **BT-BODIPY** increases greatly compared with the corresponding conformationally unrestricted BODIPYs (log ε = 4.66 for **SPh-BODIPY**, 5.09 for **BT-BODIPY**, 4.68 for **BSPh-BODIPY**, and 5.20 for **BBT-BODIPY**).

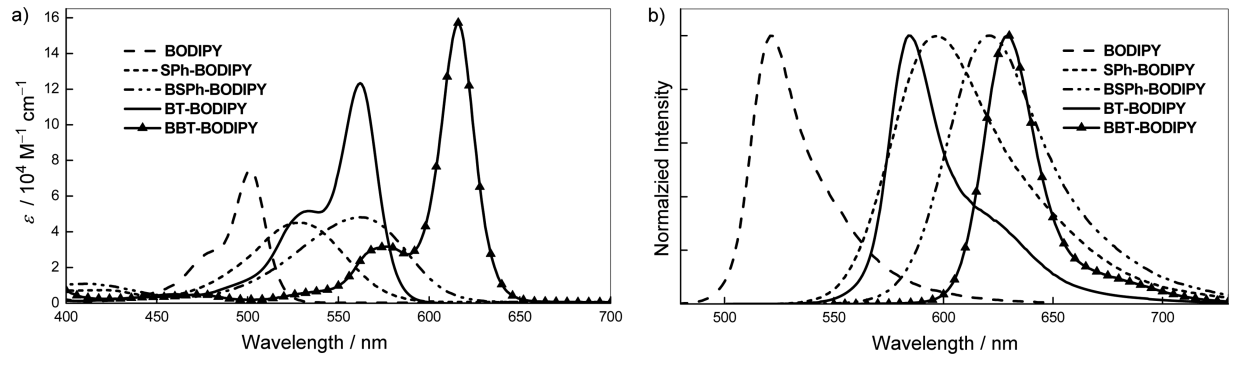

Figure 6. (a) UV−vis absorption and (b) fluorescence spectra of benzothieno[*b*]-fused BODIPYs and related compounds.

DOI: 10.1021/acs.joc.5b02531
J. Org. Chem. 2016, 81, 229−237

Table 1. UV/vis Absorption and Fluorescence Data for Benzothieno[*b*]-Fused BODIPYs and Related Compounds

	absorption		emission			excited-state dynamics		
	λ_{abs} (nm)[a]	log ε	λ_{em} (nm)	Φ_F[b]	$\Delta\lambda$ (nm)	τ (ns)	k_r (s^{-1})	k_{nr} (s^{-1})
BODIPY	501	4.87	521	0.025	20	0.24	1.0×10^8	4.1×10^9
SPh-BODIPY	528	4.66	598	0.16	70	1.87	8.6×10^7	4.4×10^8
BSPh-BODIPY	562	4.68	621	0.28	59	2.86	9.8×10^7	2.5×10^8
BT-BODIPY	562	5.09	584	0.24	22	1.93	1.2×10^8	4.0×10^8
BBT-BODIPY	616	5.20	630	0.69	14	4.91	1.4×10^8	6.0×10^7
1	658[c]	4.73[c]	673[c]	0.05[c]	15			

[a]Only the longest absorption maximum wavelengths are given. [b]Absolute quantum yields determined by a calibrated integrating sphere system. [c]Cited from ref 11a.

In the emission spectra, the **BODIPY** core exhibits a very weak green fluorescence at 521 nm (Φ_F = 0.025). Similar to the change in absorption spectra, the fluorescence is progressively red shifted by 77 and 100 nm, respectively, from **BODIPY** to **SPh-BODIPY** and **BSPh-BODIPY**, as the result of extended conjugation. The red shift of fluorescence is accompanied by the great increase in the fluorescence efficiency (Φ_F = 0.16 for **SPh-BODIPY**, 0.28 for **BSPh-BODIPY**). In addition, these two 2-(methylthio)phenyl-substituted BODIPYs show very broad emission spectra and very large Stoke shifts ($\Delta\lambda$ = 70 nm for **SPh-BODIPY**, 59 nm for **BSPh-BODIPY**), which are in contrast to typical BODIPY dyes and are supposed to be ascribed to the remarkable structural relaxation from the ground state to the excited state as the result of free rotation of the attached 2-(methylthio)phenyl. Intriguingly, the ring fusion leads to substantial increment of fluorescence efficiency (Φ_F = 0.24 for **BT-BODIPY**, 0.69 for **BBT-BODIPY**) and narrowing of fluorescence spectra, despite that the emission maxima of **BT-BODIPY** and **BBT-BODIPY** are not very different from those of **SPh-BODIPY** and **BSPh-BODIPY**. The study on the excited-state dynamics reveals that the ring fusion facilitates the radiative process while suppresses the nonradiative process. The above results clearly denote that benzothieno[*b*]-fusion is more effective than simple attachment of the 2-(methylthio)-phenyl group to enhance structure rigidity and conjugation and thus to achieve some interesting properties, including wider absorption range, high absorption coefficient and fluorescence efficiency, as well as sharp emission spectra.

In addition, the absorption and emission spectra of **BT-BODIPY** and **BBT-BODIPY** in various solvents were also measured to investigate the solvent effect. No obvious changes were observed in either absorption or emission spectra with the increase of solvent polarity (see the Supporting Information), implying that both the ground state and the excited state exhibit a small difference in the charge separation.

Moreover, we also made the comparison of the photophysical properties between **BBT-BODIPY** and **1** to illustrate the effect of ring fusion position. One big difference between these two dyes is that **1** absorbs and emits at much longer wavelengths relative to **BBT-BODIPY**. However, **1** is almost nonemissive (Φ_F = 0.05),[11a] in sharp contrast to the intense fluorescence of **BBT-BODIPY**. Considering the unique properties of **BBT-BODIPY**, intense absorption and emission in the red region, and sharp emission spectra, it may act as a promising fluorescent dye.

Electrochemical Properties. The electrochemical properties of benzothieno-fused BODIPYs and related compounds were studied by means of cyclic voltammetry. The cyclic voltammograms (CV) are shown in Figure 7. In CV diagrams, all of these molecules display a reversible reduction wave, which

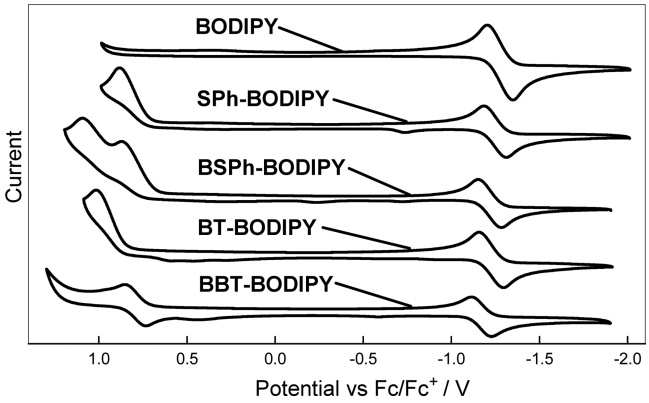

Figure 7. (a) Cyclic voltammograms of benzothieno[*b*]-fused BODIPYs and related compounds in CH_2Cl_2 (1 mM), measured with tetrabutylammonium perchlorate (0.1 M) as the supporting electrolyte at a scan rate of 100 mV/s.

should correspond to the formation of radical anion in the BODIPY core unit. As for the oxidation potential, although no oxidation wave was observed for the parent **BODIPY**, all other BODIPY dyes exhibit oxidation waves. In addition, the oxidation wave is irreversible, except for **BBT-BODIPY**. Thus, the fusion of the benzothieno ring is helpful to stabilize the formed cation radicals. On the basis of the reduction potentials, the LUMO energy levels were estimated using $E_{1/2}^{red}$ and are referenced to ferrocene, which has a HOMO of −4.8 eV. The HOMO energy levels were further estimated by subtracting the energy gap from the LUMO energy levels. The optical band gaps (E_g) were determined from the longest absorption maximum in cyclohexane. The obtained data are summarized in Table 2. All of these BODIPYs exhibit very close reduction potentials and thus LUMO energy levels, suggesting that the attachment of the 2-(methylthio)phenyl substituent as well as ring fusion has little effect on the reduction process. On

Table 2. Summary of Electrochemical Properties of Benzothieno[*b*]-Fused BODIPYs and Related Compounds[a]

	$E_{1/2}^{red}$ (eV)	LUMO level (eV)[b]	HOMO level (eV)[c]
BODIPY	−1.27	−3.53	−5.99
SPh-BODIPY	−1.24	−3.56	−5.90
BSPh-BODIPY	−1.22	−3.58	−5.84
BT-BODIPY	−1.23	−3.57	−5.83
BBT-BODIPY	−1.17	−3.63	−5.64

[a]All data are referenced versus ferrocene. [b]Values from the vacuum level were estimated by the following equation: LUMO level = −(4.8 + $E_{1/2}^{red}$/V). [c]HOMO level = LUMO level − E_g.

DOI: 10.1021/acs.joc.5b02531
J. Org. Chem. 2016, 81, 229−237

the contrary, the HOMO energy levels are greatly influenced by structure modification of the BODIPY core unit. The HOMO energy level was elevated from −5.99 eV of the parent **BODIPY** to −5.90 eV of **SPh-BODIPY** and −5.84 eV of **BSPh-BODIPY**, respectively, with the introduction of one and two 2-(methylthio)phenyl substituents. Moreover, the ring fusion leads to further elevation in HOMO energy levels. The HOMO energy level of **BT-BODIPY** is 0.07 eV higher relative to **SPh-BODIPY**. Especially, the bis(benzothieno)[*b*]-fused **BBT-BODIPY** has a HOMO 0.20 eV higher than the corresponding unstrained **BSPh-BODIPY**. These facts may be also indicative of more efficient conjugation of the ring-fused system than the corresponding unstrained one.

Theoretical Calculations. To gain a better understanding of the effect of ring fusion on the electronic structures and thus optoelectronic properties, we carried out theoretical calculations for three representative molecules, **BODIPY**, **SPh-BODIPY**, and **BT-BODIPY**. The optimization of the molecular geometry was carried out using density functional theory (DFT) calculations at B3LYP/6-31G(d). The pictorial drawings and the Kohn−Sham HOMO and LUMO energy levels are shown in Figure 8.

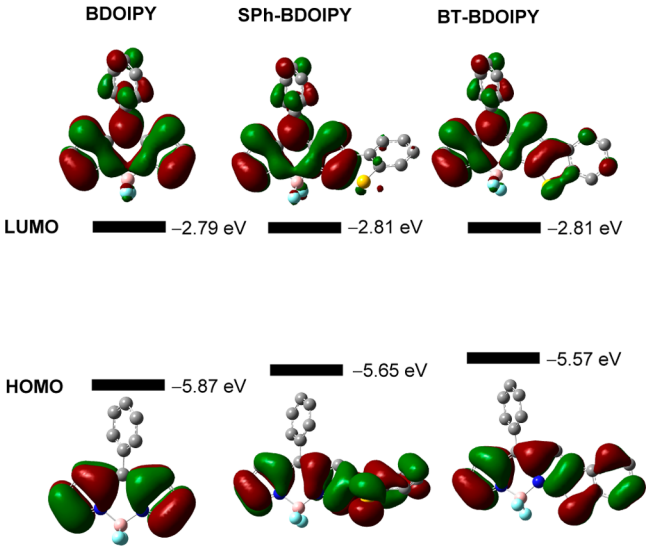

Figure 8. Pictorial presentation of the frontier orbitals and a plot of Kohn−Sham HOMO and LUMO energy levels of **BODIPY**, **SPh-BODIPY**, and **BT-BODIPY**.

The LUMO is mainly localized on the central BODIPY moiety, including the phenyl ring at the *meso*-position for all of these three BODIPY dyes. Either the contribution of 2-(methylthio)phenyl in **SPh-BODIPY** or the contribution from benzothieno in **BBT-BODIPY** is negiligle. As a result, their LUMO energy levels are almost equivalent to each other with only a 0.02 eV difference. In contrast, the HOMO can spread over the entire conjugated framework including the attched 2-(methylthio)phenyl substituent in **SPh-BODIPY** and the benzothieno moiety in **BT-BODIPY**. The extension of conjugation results in the elevation of HOMO energy level. Moreover, the HOMO of ring-fused **BT-BODIPY** lies in a substantially higher energy level compared with that of the corresponding unstrained **SPh-BODIPY**. Although there exist some discrepancies of HOMO/LUMO energy levels between calculated and experimental values, the calculated results obviously indicate that the structure modification mainly imposes substantial effects on the HOMOs. The general trend of calculated HOMO energy levels agrees well with the experimentally result, confirming that benzothieno[*b*]-fusion is more effective than simple attachment of the 2-(methylthio)-phenyl substituent in the BODIPY core to increase the HOMO energy level and thus to attain the narrow HOMO−LUMO gap as well as absorption at longer wavelength as the result of more efficient conjugation extension.

CONCLUSION

In summary, we have explored the direct synthesis of benzothieno[*b*]-fused BODIPY derivatives from methyl sulfoxide precursors, *β*-[2-(methylsulfinyl)phenyl] BODIPYs. Under concentrated H_2SO_4 conditions, the 2-(methylsulfinyl)-phenyl-substituted BODIPYs undergo both cyclization and deborylation to afford benzothieno[*b*]-fused DIPY derivatives, which can easily complex with $BF_3{\cdot}OEt_2$ to form benzothieno-[*b*]-fused BODIPYs. One advantage of this synthetic method is to make it possible to prepare asymmetric **BT-BODIPY** and symmetric **BBT-BODIPY** simultaneously, in which one and two benzothieno rings are fused, respectively. In addition, it is also possible to obtain benzothieno[*b*]-fused dipyrrins, including asymmetric **BT-DIPY**, **SOPhBT-DIPY** and symmetric **BBT-DIPY**, through this synthetic procedure. These benzothieno[*b*]-fused dipyrrins may potentially act as great ligands to prepare functional metal complexes and porphyrins. The detailed investigation on the properties revealed that the structure modification on the parent BODIPY core mainly changes electronic distribution of HOMOs, irrespective of simple attachment of the 2-(methylsulfinyl)phenyl group or fusion of the benzothieno ring. Compared with the unstrained **SPh-BODIPY** and **BSPh-BODIPY**, the conjugation in the ring-fused **BT-BODIPY** and **BBT-BODIPY** is more efficient, which results in the elevated HOMO energy levels and thus red shift in absorption. In addition, the ring-fused **BT-BODIPY** and **BBT-BODIPY** exhibit better absorptivity and higher fluorescence efficiency. Furthermore, the ring fusion is helpful to stabilize the formed cation in **BBT-BODIPY**. Considering the intriguing properties of **BBT-BODIPY**, such as intense absorption and emission in the red region, very sharp emission spectra, and reversible oxidation and reduction potentials, it may find some potential applications as promising emitting or bipolar transporting materials. Further researches along this line are underway in our group.

EXPERIMENTAL SECTION

General. ^1H spectra were recorded at 300/400 MHz, and ^{13}C NMR spectra were measured at 75/100 MHz in $CDCl_3$. High-resolution mass spectra (HRMS) were obtained using an electrospray ionization time-of-flight (ESI-TOF) mass spectrometer for **BT-DIPY**, **SOPhBT-DIPY**, and **BBT-DIPY** and a matrix-assisted laser desorption/ionization Fourier transform ion cyclotron resonance (MALDI-FTICR) spectrometer for other compounds. All reactions were carried out under a nitrogen atmosphere. **2-BromoBODIPY** and **2,6-dibromoBODIPY** were prepared according to the literature.[19]

Computational Methods. All calculations are conducted by using the Gaussian 09 program.[22] The geometries in the ground state were optimized using density functional theory (DFT) at the B3LYP/6-31G(d) level of theory. The NICS values were obtained with the gauge-independent atomic orbital (GIAO) method at the B3LYP/6-31++G(d,p) level of theory.

SPh-BODIPY: To a solution of **2-bromoBODIPY** (867 mg, 2.5 mmol), 2-thioanisoleboronic acid (504 mg, 3.0 mmol), and $Pd(PPh_3)_4$ (144 mg, 0.125 mmol) in degassed toluene (60 mL) was added a

DOI: 10.1021/acs.joc.5b02531
J. Org. Chem. 2016, 81, 229−237

degassed solution of K_2CO_3 (6 mL, 2.0 M) under a steam of nitrogen. After the reaction mixture was refluxed overnight, the mixture was cooled to room temperature and then extracted with CH_2Cl_2. The combined organic layer was dried over anhydrous Na_2SO_4, filtered, and concentrated under reduced pressure. The resulting mixture was subjected to a silica gel column chromatography (4/1 petroleum ether/CH_2Cl_2, R_f = 0.45) to afford 721 mg (1.85 mmol) of **SPh-BODIPY** in 74% yield as dark red solids. mp 128.5−130.5 °C; ^{1}H NMR ($CDCl_3$, 300 MHz): δ 2.43 (s, 3H), 6.56 (d, J = 3.3 Hz, 1H), 6.94 (d, J = 3.6 Hz, 1H), 7.12−7.18 (m, 2H), 7.27−7.29 (m, 3H), 7.51−7.64 (m, 5H), 7.96 (s, 1H), 8.26 (s, 1H); ^{13}C NMR ($CDCl_3$, 75 MHz): δ 16.2, 118.4, 125.1, 126.0, 128.3, 128.5, 129.4, 130.1, 130.6, 130.8, 131.4, 132.1, 132.8, 133.9, 134.9, 135.1, 137.2, 143.9, 144.7, 147.0, HRMS (MALDI-FTICR): 389.1206 (M^+); Calcd for $C_{22}H_{17}{}^{10}BF_2N_2S$: 389.1204.

SOPh-BODIPY. **SPh-BODIPY** (195 mg, 0.50 mmol) was first dissolved in a 2:1 mixture of glacial acetic acid and chloroform (2:1) and then cooled with an ice bath until the solvent was about to freeze. Hydrogen peroxide (30%, 0.1 mL, 1 mmol) was added slowly. The cooling bath was removed, and the mixture was stirred at room temperature for 12 h. After acetic acid was removed by vacuum evaporation, CH_2Cl_2 was added to the residue. The organic fraction was washed with saturated $NaHCO_3$ solution, dried over Na_2SO_4, filtered, and concentrated under reduced pressure. The resulting mixture was subjected to a silica gel column chromatography (ethyl acetate, R_f = 0.35) to afford 203 mg (0.5 mmol) of **SOPh-BODIPY** in 100% yield as red solids. mp 114.5−116.5 °C; ^{1}H NMR ($CDCl_3$, 400 MHz): δ 2.53 (s, 3H), 6.63 (d, J = 4.0 Hz, 1H), 7.03−7.05 (m, 2H), 7.37 (dd, J = 1.2, 7.6 Hz, 1H), 7.48 (td, J = 1.6, 7.6 Hz, 1H), 7.55−7.66 (m, 6H), 8.02 (d, J = 13.2 Hz, 2H), 8.09 (dd, J = 1.2, 8.0 Hz 1H); ^{13}C NMR ($CDCl_3$, 75 MHz): δ 42.1, 119.7, 123.7, 128.7, 128.9, 129.1, 129.4, 129.7, 130.5, 130.8, 131.1, 131.3, 133.1, 133.4, 134.9, 135.7, 141.6, 143.9, 146.3, 147.9.

BT-DIPY. **SOPh-BODIPY** (200 mg, 0.49 mmol) was added in portions to stirred concentrated H_2SO_4 (0.6 mL, 3 v/w) in a one-neck, round-bottom flask at 0−5 °C. After the reaction mixture was stirred at room temperature for 5 min, the reaction mixture was poured on ice-cold water and then made basic with aqueous potassium carbonate solution (pH = 8). The aqueous layer was extracted with CH_2Cl_2. The combined organic layer was dried over anhydrous Na_2SO_4, filtered, and concentrated under reduced pressure. The resulting mixture was subjected to a silica gel column chromatography (4/1 petroleum ether/CH_2Cl_2, R_f = 0.38) to afford 63 mg (0.19 mmol) of **BT-DIPY** in 39% yield as purple solids. mp 163.5−165.5 °C; ^{1}H NMR ($CDCl_3$, 300 MHz): δ 6.28 (dd, J = 2.7, 3.9 Hz, 1H), 6.37 (dd, J = 0.9, 3.9 Hz, 1H), 6.84 (s, 1H), 7.17−7.28 (m, 2H), 7.31 (s, 1H), 7.44−7.58 (m, 7H), 12.75 (br, 1H); ^{13}C NMR ($CDCl_3$, 100 MHz): δ 111.8, 122.5, 123.2, 123.5, 124.2, 125.5, 126.1, 127.6, 127.7, 128.6, 128.9, 129.7, 131.2, 133.4, 135.6, 137.2, 139.5, 140.8, 143.4; HRMS (ESI-TOF): 327.0955 $[M + H]^+$; Calcd for $C_{21}H_{14}N_2S$: 327.0956.

BT-BODIPY. To a solution of **BT-DIPY** (100 mg,0.3 mmol) in anhydrous dichloromethane (15 mL) was added triethylamine (5 mL) under nitrogen. After the solution was stirred for 15 min at room temperature, $BF_3{\cdot}OEt_2$ (7 mL) was added. The mixture was stirred at room temperature overnight. The mixture was washed with water and then extracted with CH_2Cl_2. The combined organic layer was dried over anhydrous Na_2SO_4, filtered, and concentrated under reduced pressure. The resulting mixture was subjected to a silica gel column chromatography (2/1 petroleum ether/CH_2Cl_2, R_f = 0.42) to afford 108 mg (0.28 mmol) of **BT-BODIPY** in 94% yield as dark red solids. mp 190.3−192.6 °C; ^{1}H NMR ($CDCl_3$, 300 MHz): δ 6.53 (dd, J = 3.9, 1.8 Hz, 1H), 6.86 (d, J = 3.9 Hz, 1H), 7.11 (s, 1H), 7.32−7.37 (m, 2H), 7.54−7.64 (m, 5H), 7.67−7.73 (m, 2H), 7.89 (s, 1H); ^{13}C NMR ($CDCl_3$, 100 MHz): δ 118.0, 120.4, 122.6, 124.3, 125.9, 126.9, 128.5, 129.2, 129.9, 130.6, 130.7, 133.8, 135.2, 135.8, 140.2, 141.7, 142.2, 144.7, 161.3; HRMS (MALDI-FTICR): 373.0894 (M^+); Calcd for $C_{21}H_{13}{}^{10}BF_2N_2S$: 373.0891.

BSPh-BODIPY. This compound was prepared essentially in the same manner as that described for **SPh-BODIPY** using **2,6-dibromoBODIPY** (426 mg, 1.0 mmol), $Pd(OAc)_2$ (23.0 mg, 0.1 mmol), X-Phos (95.0 mg, 0.2 mol), 2-thioanisoleboronic acid (370 mg, 2.2 mmol), Cs_2CO_3 (652 mg, 2.0 mmol), 1,4-dioxane (30 mL), and H_2O (6 mL). The mixture was stirred at room temperature for 48 h. The purification by silica gel column chromatography (2/1 petroleum ether/CH_2Cl_2, R_f = 0.50) afforded 450 mg (0.88 mmol) of **BSPh-BODIPY** in 88% yield as purple solids. mp 203.3−205.5 °C; ^{1}H NMR ($CDCl_3$, 300 MHz): δ 2.44 (s, 6H), 7.13 (s, 2H), 7.16−7.18 (m, 2H), 7.27−7.31 (m, 6H), 7.52−7.59 (m, 3H), 7.66 (d, J = 7.5 Hz, 2H), 8.27 (s, 2H); ^{13}C NMR ($CDCl_3$, 75 MHz): δ 16.2, 125.1, 126.1, 128.3, 128.5, 129.4, 129.9, 130.6, 130.8, 132.2, 132.7, 133.9, 135.0, 137.2, 144.5 146.6; HRMS (MALDI-FTICR): 511.1392 (M^+); Calcd for $C_{29}H_{23}{}^{10}BF_2N_2S_2$: 511.1395.

BSOPh-BODIPY. This compound was prepared essentially in the same manner as that described for **SOPh-BODIPY** using **BSPh-BODIPY**(2.31 g, 4.5 mmol), a 2:1 mixture of glacial acetic acid and chloroform (36 mL), and hydrogen peroxide (30%, 1.1 mL, 11 mmol). The purification by silica gel column chromatography (ethyl acetate, R_f = 0.25) afforded 2.21 g (4.06 mmol) of **BSOPh-BODIPY** in 90% yield as red solids. mp 257.0−258.0 °C; ^{1}H NMR ($CDCl_3$, 300 MHz): δ 2.56 (s, 6H), 7.11 (s, 2H), 7.38 (dd, J = 0.9, 7.5 Hz, 2H), 7.50 (td, J = 1.2, 7.5 Hz, 2H), 7.58−7.67 (m, 7H), 8.11−8.14 (m, 4H); ^{13}C NMR ($CDCl_3$, 75 MHz): δ 42.3, 123.8, 128.9, 129.4, 129.6, 130.2, 130.4, 130.5, 131.2, 131.7, 133.1, 135.6, 143.8, 144.2, 148.6.

SOPhBT-DIPY. This compound was prepared essentially in the same manner as that described for **BT-DIPY** using **BSOPh-BODIPY** (2.21 g, 4.06 mmol) and concentrated H_2SO_4 (6.6 mL, 3 v/w). The purification by silica gel column chromatography (ethyl acetate, R_f = 0.25) afforded 1.58 g (3.40 mmol) of **SOPhBT-DIPY** in 84% yield as purple solids. mp 149.5−151.5 °C; ^{1}H NMR ($CDCl_3$, 300 MHz): δ 2.50 (s, 3H), 6.45 (d, J = 1.5 Hz, 1H), 6.86 (s, 1H), 7.19−7.29 (m, 2H), 7.32 (dd, J = 1.5, 7.5 Hz, 1H), 7.41−7.59 (m, 10H), 8.03 (dd, J = 1.5, 7.5 Hz, 1H), 12.93 (br, 1H); ^{13}C NMR ($CDCl_3$, 75 MHz): δ 41.7, 120.8, 123.2, 123.3, 123.6, 123.8, 124.3, 125.6, 126.8, 127.9, 128.0, 128.1, 129.2, 129.4, 129.8, 130.7, 131.1, 132.4, 134.3, 136.7, 139.6, 140.5, 143.4, 143.7, 154.2, 174.9; HRMS (ESI-TOF): 465.1098 $[M + H]^+$; Calcd for $C_{28}H_{20}N_2OS_2$: 465.1095.

SOPhBT-BODIPY. This compound was prepared essentially in the same manner as that described for **BT-BODIPY** using **SOPhBT-DIPY** (1.55 g, 3.4 mmol), anhydrous dichloromethane (100 mL), triethylamine (17 mL), and $BF_3{\cdot}OEt_2$ (22 mL). The purification by silica gel chromatography (ethyl acetate, R_f = 0.28) afforded 1.61 g (3.14 mmol) of **SOPhBT-BODIPY** in 92% yield as dark red solids. mp 274.5−276.5 °C; ^{1}H NMR ($CDCl_3$, 300 MHz): δ 2.55 (s, 3H), 6.93 (s, 1H), 7.17 (s, 1H), 7.36−7.41 (m, 3H), 7.47−7.76 (m, 9H), 7.94 (s, 1H), 8.08 (dd, J = 1.2, 7.5 Hz, 1H); ^{13}C NMR ($CDCl_3$, 75 MHz): δ 42.1, 121.2, 122.9, 123.6, 124.4, 126.2, 127.0, 127.6, 128.7, 128.8, 129.6, 130.6, 130.9, 130.9, 131.1, 133.4, 135.2, 137.1, 139.4, 141.0, 141.8, 143.9, 144.0, 144.5, 163.8; HRMS (MALDI-FTICR): 511.1035 (M^+); Calcd for $C_{28}H_{19}{}^{10}BF_2N_2OS_2$: 511.1031.

BBT-DIPY. This compound was prepared essentially in the same manner as that described for **BT-DIPY** using **SOPhBT-BODIPY** (1.53 g, 3 mmol) and concentrated H_2SO_4 (4.6 mL, 3 v/w). The purification by silica gel column chromatography (2/1 petroleum ether/CH_2Cl_2, R_f = 0.48) afforded 660 mg (1.53 mmol) of **BBT-DIPY** in 51% yield as dark green solids. mp > 300 °C; ^{1}H NMR ($CDCl_3$, 300 MHz): δ 6.78 (s, 2H), 7.26−7.30 (m, 4H), 7.55−7.66 (m, 9H), 13.91 (br, 1H); ^{13}C NMR ($CDCl_3$, 75 MHz): δ 117.6, 121.4, 123.1, 124.4, 125.1, 126.8, 128.2, 129.1, 130.3, 133.3, 135.7, 140.6, 157.5; HRMS (ESI-TOF): 433.0827 $[M + H]^+$; Calcd for $C_{27}H_{16}N_2S_2$: 433.0833.

BBT-BODIPY. This compound was prepared essentially in the same manner as that described for **BT-BODIPY** using **BBT-DIPY** (580 mg, 1.3 mmol), anhydrous dichloromethane (50 mL), triethylamine (7 mL), and $BF_3{\cdot}OEt_2$ (9 mL). The purification by silica gel column chromatography (2/1 petroleum ether/CH_2Cl_2, R_f = 0.33) afforded 580 mg (1.21 mmol) of **BBT-BODIPY** in 93% yield as dark green solids. mp > 300 °C; ^{1}H NMR ($CDCl_3$, 300 MHz): δ 7.04 (s, 2H), 7.31−7.37 (m, 4H), 7.57−7.69 (m, 3H), 7.70−7.75 (m, 6H); ^{13}C NMR ($CDCl_3$, 75 MHz): δ 117.9, 121.4, 123.3, 124.8, 125.6, 127.6, 128.4, 129.4, 129.8, 132.7, 134.3, 139.5, 140.7, 141.2, 158.4; HRMS

DOI: 10.1021/acs.joc.5b02531
J. Org. Chem. 2016, 81, 229−237

(MALDI-FTICR): 479.0778 (M^+); Calcd for $C_{27}H_{15}{}^{10}BF_2N_2S_2$: 479.0769.

X-ray Crystal-Structure Analysis. Single crystals of **BT-DIPY**, **SOPhBT-DIPY**, **BT-BODIPY**, and **BBT-BODIPY** were obtained by recrystallization from dichloromethane/*n*-hexane. Data were collected on a Bruker SMART CCD X-ray diffractometer (APEX II) with Mo Kα radiation (λ = 0.71073 Å) and a graphite monochromator. The structures were solved by direct methods (SHELEX-97) and refined by the full-matrix least-squares methods on F^2 (SHELXL-97).[23] CCDC 1432234 (**BT-DIPY**), 1432235 (**SOPh-DIPY**), 1432233 (**BT-BODIPY**), and 1432232 (**BBT-BODIPY**) contain the supplementary crystallographic data for this paper. These data can be obtained free of charge from The Cambridge Crystallographic Data Centre via www.ccdc.cam.ac.uk/data_request/cif.

■ ASSOCIATED CONTENT

Supporting Information

The Supporting Information is available free of charge on the ACS Publications website at DOI: 10.1021/acs.joc.5b02531.

UV−vis absorption and fluorescence spectra of **BT-BODIPY** and **BBT-BODIPY** in various solvents, ^{1}H NMR and ^{13}C NMR of all new compounds, energy and Cartesian coordinates table for **BODIPY**, **SPh-BODIPY**, and **BT-BODIPY** (PDF)

Crystallographic data of **BT-DIPY** (CIF)

Crystallographic data of **SOPhBT-DIPY** (CIF)

Crystallographic data of **BT-BODIPY** (CIF)

Crystallographic data of **BBT-BODIPY** (CIF)

■ AUTHOR INFORMATION

Corresponding Author

*E-mail: chzhao@sdu.edu.cn.

Notes

The authors declare no competing financial interest.

■ ACKNOWLEDGMENTS

This work was supported by the National Nature Science Foundation of China (Nos. 21272141, 21572120) and the Distinguished Middle-Aged and Young Scientist Encourage and Reward Foundation of Shandong Province (No. BS 2012CL021).

■ REFERENCES

(1) For reviews of BODIPYs dyes, see: (a) Bessette, A.; Hanan, G. S. *Chem. Soc. Rev.* **2014**, *43*, 3342−3405. (b) Lu, H.; Mack, J.; Yang, Y.; Shen, Z. *Chem. Soc. Rev.* **2014**, *43*, 4778−4823. (c) Loudet, A.; Burgess, K. *Chem. Rev.* **2007**, *107*, 4891−4932. (d) Ulrich, G.; Ziessel, R.; Harriman. *Angew. Chem., Int. Ed.* **2008**, *47*, 1184−1201. (e) Kamkaew, A.; Lim, S. H.; Lee, H. B.; Kiew, L. V.; Chung, L. Y.; Burgess, K. *Chem. Soc. Rev.* **2013**, *42*, 77−88.

(2) (a) Wang, F.; Zhou, L.; Zhao, C.; Wang, R.; Fei, Q.; Luo, S.; Guo, Z.; Tian, H.; Zhu, W.-H. *Chem. Sci.* **2015**, *6*, 2584−2589. (b) Xu, W.; Bai, J.; Peng, J.; Samanta, A.; Divyanshu; Chang, Y.-T. *Chem. Commun.* **2014**, *50*, 10398−10401. (c) Juarez, L. A.; Costero, A. M.; Parra, M.; Gil, S.; Sancenon, F.; Martinez-Manez, R. *Chem. Commun.* **2015**, *51*, 1725−1727. (d) Salim, M. M.; Owens, E. A.; Gao, T.; Lee, J. H.; Hyun, H.; Choi, H. S.; Henary, M. *Analyst* **2014**, *139*, 4862−4873. (e) Niu, L. Y.; Guan, Y. S.; Chen, Y. Z.; Wu, L. Z.; Tung, C. H.; Yang, Q. Z. *J. Am. Chem. Soc.* **2012**, *134*, 18928−18931. (f) Wang, H.; Wu, Y.; Shi, Y.; Tao, P.; Fan, X.; Su, X.; Kuang, G. C. *Chem. - Eur. J.* **2015**, *21*, 3219−3223. (g) Hu, J. J.; Wong, N. K.; Gu, Q.; Bai, X.; Ye, S.; Yang, D. *Org. Lett.* **2014**, *16*, 3544−3547.

(3) (a) Yogo, T.; Urano, Y.; Ishitsuka, Y.; Maniwa, F.; Nagano, T. *J. Am. Chem. Soc.* **2005**, *127*, 12162−12163. (b) Ozlem, S.; Akkaya, E. U. *J. Am. Chem. Soc.* **2009**, *131*, 48−49.

(4) (a) Xiao, Y.; Zhang, D.; Qian, X.; Costela, A.; Garcia-Moreno, I.; Martin, V.; Perez-Ojeda, M. E.; Banuelos, J.; Gartzia, L.; Arbeloa, I. L. *Chem. Commun.* **2011**, *47*, 11513−11515. (b) Duran-Sampedro, G.; Esnal, I.; Agarrabeitia, A. R.; Banuelos Prieto, J.; Cerdan, L.; Garcia-Moreno, I.; Costela, A.; Lopez-Arbeloa, I.; Ortiz, M. J. *Chem. - Eur. J.* **2014**, *20*, 2646−2653. (c) Liras, M.; Bañuelos Prieto, J.; Pintado-Sierra, M.; García-Moreno, I.; Costela, Á.; Infantes, L.; Sastre, R.; Amat-Guerri, F. *Org. Lett.* **2007**, *9*, 4183−4186.

(5) (a) Liu, C.-L.; Chen, Y.; Shelar, D. P.; Li, C.; Cheng, G.; Fu, W.-F. *J. Mater. Chem. C* **2014**, *2*, 5471. (b) Bonardi, L.; Kanaan, H.; Camerel, F.; Jolinat, P.; Retailleau, P.; Ziessel, R. *Adv. Funct. Mater.* **2008**, *18*, 401−413.

(6) (a) Bura, T.; Leclerc, N.; Fall, S.; Leveque, P.; Heiser, T.; Retailleau, P.; Rihn, S.; Mirloup, A.; Ziessel, R. *J. Am. Chem. Soc.* **2012**, *134*, 17404−17407. (b) Lefebvre, J. F.; Sun, X. Z.; Calladine, J. A.; George, M. W.; Gibson, E. A. *Chem. Commun.* **2014**, *50*, 5258−5260. (c) Lin, H. Y.; Huang, W. C.; Chen, Y. C.; Chou, H. H.; Hsu, C. Y.; Lin, J. T.; Lin, H. W. *Chem. Commun.* **2012**, *48*, 8913−8915. (d) Kolemen, S.; Bozdemir, O. A.; Cakmak, Y.; Barin, G.; Erten-Ela, S.; Marszalek, M.; Yum, J.-H.; Zakeeruddin, S. M.; Nazeeruddin, M. K.; Grätzel, M.; Akkaya, E. U. *Chem. Sci.* **2011**, *2*, 949.

(7) (a) Schmidt, E. Yu.; Zorina, N. V.; Dvorko, M. Yu.; Protsuk, N. I.; Belyaeva, K. V.; Clavier, G.; Meallet-Renault, R.; Vu, T. T.; Mikhaleva, A. I.; Trofimov, B. A. *Chem.—Eur. J.* **2011**, *17*, 3069−3073. (b) Sobenina, L. N.; Vasil'tsov, A. M.; Petrova, O. V.; Petrushenko, K. B.; Ushakov, I. A.; Clavier, G.; Meallet-Renault, R.; Mikhaleva, A. I.; Trofimov, B. A. *Org. Lett.* **2011**, *13*, 2524−2527.

(8) (a) Lu, H.; Wang, Q.; Gai, L.; Li, Z.; Deng, Y.; Xiao, X.; Lai, G.; Shen, Z. *Chem. - Eur. J.* **2012**, *18*, 7852−7861. (b) Fu, G.-L.; Pan, H.; Zhao, Y.-H.; Zhao, C. H. *Org. Biomol. Chem.* **2011**, *9*, 8141−8146.

(9) (a) Ziessel, R.; Rihn, S.; Harriman, A. *Chem. - Eur. J.* **2010**, *16*, 11942−11953. (b) Qu, X.; Liu, Q.; Ji, X.; Chen, H.; Zhou, Z.; Shen, Z. *Chem. Commun.* **2012**, *48*, 4600−4602.

(10) (a) Killoran, J.; Allen, L.; Gallagher, J. F.; Gallagher, W. M.; O'Shea, D. F. *Chem. Commun.* **2002**, 1862−1863. (b) McDonnell, S. O.; O'Shea, D. F. *Org. Lett.* **2006**, *8*, 3493−3496. (c) Zhao, W.; Carreira, E. M. *Angew. Chem., Int. Ed.* **2005**, *44*, 1677−1679. (d) Shimizu, S.; Iino, T.; Saeki, A.; Seki, S.; Kobayashi, N. *Chem. - Eur. J.* **2015**, *21*, 2893−2904. (e) Liu, H.; Lu, H.; Zhou, Z.; Shimizu, S.; Li, Z.; Kobayashi, N.; Shen, Z. *Chem. Commun.* **2015**, *51*, 1713−1716.

(11) (a) Chen, J.; Burghart, A.; Derecskei-Kovacs, A.; Burgess, K. *J. Org. Chem.* **2000**, *65*, 2900−2906. (b) Umezawa, K.; Nakamura, Y.; Makino, H.; Citterio, D.; Suzuki, K. *J. Am. Chem. Soc.* **2008**, *130*, 1550−1551. (c) Umezawa, K.; Matsui, A.; Nakamura, Y.; Citterio, D.; Suzuki, K. *Chem. - Eur. J.* **2009**, *15*, 1096−1106. (d) Awuah, S. G.; Polreis, J.; Biradar, V.; You, Y. *Org. Lett.* **2011**, *13*, 3884−3887. (e) Yu, C.; Xu, Y.; Jiao, L.; Zhou, J.; Wang, Z.; Hao, E. *Chem. - Eur. J.* **2012**, *18*, 6437−6442. (f) Ni, Y.; Zeng, W.; Huang, K.-W.; Wu, J. *Chem. Commun.* **2013**, *49*, 1217−1219. (g) Wakamiya, A.; Murakami, T.; Yamaguchi, S. *Chem. Sci.* **2013**, *4*, 1002−1007. (h) Wu, Y.; Cheng, C.; Jiao, L.; Yu, C.; Wang, S.; Wei, Y.; Mu, X.; Hao, E. *Org. Lett.* **2014**, *16*, 748−751. (i) Wang, J.; Wu, Q.; Wang, S.; Yu, C.; Li, J.; Hao, E.; Wei, Y.; Mu, X.; Jiao, L. *Org. Lett.* **2015**, *17*, 5360−5363.

(12) Leen, V.; Qin, W.; Yang, W.; Cui, J.; Xu, C.; Tang, X.; Liu, W.; Robeyns, K.; Van Meervelt, L.; Beljonne, D.; Lazzaroni, R.; Tonnele, C.; Boens, N.; Dehaen, W. *Chem. - Asian J.* **2010**, *5*, 2016−2026.

(13) (a) Jiao, C.; Huang, K.-W.; Wu, J. *Org. Lett.* **2011**, *13*, 632−635. (b) Jiao, C.; Zhu, L.; Wu, J. *Chem. - Eur. J.* **2011**, *17*, 6610−6614.

(14) Hayashi, Y.; Obata, N.; Tamaru, M.; Yamaguchi, S.; Matsuo, Y.; Saeki, A.; Seki, S.; Kureishi, Y.; Saito, S.; Yamaguchi, S.; Shinokubo, H. *Org. Lett.* **2012**, *14*, 866−869.

(15) Heyer, E.; Retailleau, P.; Ziessel, R. *Org. Lett.* **2014**, *16*, 2330−2333.

(16) Luo, L.; Wu, D.; Li, W.; Zhang, S.; Ma, Y.; Yan, S.; You, J. *Org. Lett.* **2014**, *16*, 6080−6083.

(17) Zhou, X.; Wu, Q.; Feng, Y.; Yu, Y.; Yu, C.; Hao, E.; Wei, Y.; Mu, X.; Jiao, L. *Chem.—Asian J.* **2015**, *10*, 1979−1986.

(18) (a) Gao, P.; Beckmann, D.; Tsao, H. N.; Feng, X.; Enkelmann, V.; Pisula, W.; Mullen, K. *Chem. Commun.* **2008**, 1548−1550. (b) Gao,

DOI: 10.1021/acs.joc.5b02531
J. Org. Chem. 2016, 81, 229−237

J.; Li, Y.; Wang, Z. *Org. Lett.* **2013**, *15*, 1366−1369. (c) Zhang, S.; Qiao, X.; Chen, Y.; Wang, Y.; Edkins, R. M.; Liu, Z.; Li, H.; Fang, Q. *Org. Lett.* **2014**, *16*, 342−345. (d) Pandya, V. B.; Jain, M. R.; Chaugule, B. V.; Patel, J. S.; Parmar, B. M.; Joshi, J. K.; Patel, P. R. *Synth. Commun.* **2012**, *42*, 497−505. (e) Chen, D. M.; Wang, S.; Li, H. X.; Zhu, X. Z.; Zhao, C. H. *Inorg. Chem.* **2014**, *53*, 12532−12539.

(19) Jiao, L.; Pang, W.; Zhou, J.; Wei, Y.; Mu, X.; Bai, G.; Hao, E. *J. Org. Chem.* **2011**, *76*, 9988−9996.

(20) (a) Wood, T. E.; Thompson, A. *Chem. Rev.* **2007**, *107*, 1831−1861. (b) Muldoon, M. J. *Dalton. Trans.* **2010**, *39*, 337−348.

(21) (a) Crawford, S. M.; Thompson, A. *Org. Lett.* **2010**, *12*, 1424−1427. (b) Smithen, D. A.; Baker, A. E.; Offman, M.; Crawford, S. M.; Cameron, T. S.; Thompson, A. *J. Org. Chem.* **2012**, *77*, 3439−3453. (c) Tahtaoui, C.; Thomas, C.; Rohmer, F.; Klotz, P.; Duportail, G.; Mély, Y.; Bonnet, D.; Hibert, M. *J. Org. Chem.* **2007**, *72*, 269−272. (d) Lundrigan, T.; Cameron, T. S.; Thompson, A. *Chem. Commun.* **2014**, *50*, 7028−7031.

(22) Frisch, M. J.; Trucks, G. W.; Schlegel, H. B.; Scuseria, G. E.; Robb, M. A.; Cheeseman, J. R.; Scalmani, G.; Barone, V.; Mennucci, B.; Petersson, G. A.; Nakatsuji, H.; Caricato, M.; Li, X.; Hratchian, H. P.; Izmaylov, A. F.; Bloino, J.; Zheng, G.; Sonnenberg, J. L.; Hada, M.; Ehara, M.; Toyota, K.; Fukuda, R.; Hasegawa, J.; Ishida, M.; Nakajima, T.; Honda, Y.; Kitao, O.; Nakai, H.; Vreven, T.; Montgomery, J. A., Jr.; Peralta, J. E.; Ogliaro, F.; Bearpark, M.; Heyd, J. J.; Brothers, E.; Kudin, K. N.; Staroverov, V. N.; Keith, T.; Kobayashi, R.; Normand, J.; Raghavachari, K.; Rendell, A.; Burant, J. C.; Iyengar, S. S.; Tomasi, J.; Cossi, M.; Rega, N.; Millam, J. M.; Klene, M.; Knox, J. E.; Cross, J. B.; Bakken, V.; Adamo, C.; Jaramillo, J.; Gomperts, R.; Stratmann, R. E.; Yazyev, O.; Austin, A. J.; Cammi, R.; Pomelli, C.; Ochterski, J. W.; Martin, R. L.; Morokuma, K.; Zakrzewski, V. G.; Voth, G. A.; Salvador, P.; Dannenberg, J. J.; Dapprich, S.; Daniels, A. D.; Farkas, O.; Foresman, J. B.; Ortiz, J. V.; Cioslowski, J.; Fox, D. J. *Gaussian 09*, Revision B.01; Gaussian, Inc.: Wallingford, CT, 2010.

(23) Sheldrick, G. M. *SHELXL-97: Program for the Refinement of Crystal Structure*; University of Göttingen: Göttingen, Germany, 1997.

DOI: 10.1021/acs.joc.5b02531
J. Org. Chem. 2016, 81, 229−237